American Mineralogist, Volume 92, pages 691–694, 2007

LETTER

Ion microprobe analysis of (^{231}Pa)/(^{235}U) and an appraisal of protactinium partitioning in igneous zircon

AXEL K. SCHMITT*

Department of Earth and Space Sciences, University of California, Los Angeles, California 90095, U.S.A.

ABSTRACT

Ion microprobe U-Pa measurements in zircon crystals from a Holocene rhyolite (Salton Buttes, California) are utilized to assess the partitioning of Pa and U between zircon and melt. The relative sensitivity factor (RSF) for ion microprobe U-Pa zircon analysis was calibrated on a natural high-U secular equilibrium zircon from Buff Peak (Nevada). Zircon crystals from Salton Buttes rhyolite show evidence for excess ^{231}Pa with a weighted average (^{231}Pa)/(^{235}U) activity ratio of 1.9. From this ratio, model zircon-melt partition coefficient ratios $D_{Pa}/D_U = 0.9–2.2$ are obtained, assuming plausible limits for $(^{231}Pa)/(^{235}U)_{melt}$ and correcting for the age of zircon crystallization (~15 ka). These values roughly fit lattice strain models for tetravalent cations, but are more than one order of magnitude lower than predictions for pentavalent Pa. Based on this appraisal of Pa partitioning, initial ^{231}Pa disequilibrium caused by zircon-melt fractionation alone can produce minor discordance or excess ^{207}Pb in Late Cenozoic zircon, but is insignificant for older U-Pb zircon ages.

Keywords: Pa-231, zircon, partition coefficients, uranium disequilibrium, rhyolites

INTRODUCTION

Zircon is of paramount importance for geochronology based on its preference for actinide elements while excluding initial Pb, its chemical and physical stability, and slow diffusion of radioactive parents and daughters. It is amenable to multiple dating methods, including U-Pb, Th-Pb, U-Th-He, radiation damage, and U-series disequilibrium. Disequilibrium between long-lived intermediate daughters ^{230}Th (half-life t½ = 75 690 a) or ^{231}Pa (t½ = 32 760 a) and their respective parents ^{238}U (magmatic fractionation between ^{234}U and ^{238}U assumed negligible) and ^{235}U ultimately impacts the abundance of radiogenic ^{206}Pb, ^{207}Pb, and He, and requires corrections for accurate age determination (e.g., Mattinson 1973). Zircon favors U over Th with a zircon-melt partitioning coefficient ratio D_U/D_{Th} ~6 (e.g., Blundy and Wood 2003) so that initial $(^{230}Th)/(^{238}U)_{zircon}$ (activities denoted by parentheses) is expected to be ~0.17. The resulting ^{206}Pb deficit is practically negligible within analytical precision for zircon crystals older than ~100 Ma and even for complete exclusion of initial ^{230}Th can only amount to a ~108 ka age difference (Schärer 1984). By contrast, excess ^{231}Pa has been frequently invoked as a source for strong ^{207}Pb excesses in Pre-Quaternary or even Archean zircon crystals, including those of the oldest known terrestrial zircon (e.g., Anczkiewicz et al. 2001; Parrish and Noble 2003; cf. Wilde et al. 2001). In theory, the incorporation of strong ^{231}Pa excesses in zircon could significantly affect even old ^{207}Pb/^{235}U and ^{207}Pb/^{206}Pb ages.

Lattice strain models for zircon-melt partitioning of Pa^{5+} (Fig. 1; Blundy and Wood 2003) are based on estimates for Nb^{5+} as a proxy for Pa^{5+}. Published $D_{Nb} = 0.34$ and lattice strain parameters (apparent Young's modulus $E^{5+} > E^{4+} = 750$ GPa and site radius $r_0^{4+} = r_0^{5+} = 0.91$ Å; Blundy and Wood 2003) imply that the parabola for 5+ cations should be similar to the 4+ curve, and consequently Pa^{5+} is expected to be highly compatible in zircon ($D_{Pa}/D_U > 30$; Fig. 1). Direct experimental constraints on zircon-melt partitioning of Pa, however, are lacking. The low abundance of ^{231}Pa, high radioactivity and toxicity, and the absence of a stable Pa isotope impose such analytical and experimental challenges that Parrish and Noble (2003) commented that the ^{231}Pa isotope effects in accessory minerals "can be inferred only by the measurements of the decay products of ^{231}Pa, not to the measurement of ^{231}Pa directly" (p. 205). Here, I introduce a high-sensitivity and high-spatial resolution secondary ionization mass spectrometry (SIMS, ion microprobe) method for the direct determination of ^{231}Pa in zircon. By applying this technique to young zircon crystals from a rhyolite with a Holocene eruption age, the first observational constraints on zircon-melt partitioning of Pa relative to U are obtained.

METHODS

Hand-picked zircon grains (typically 100–150 µm long) were epoxy-mounted, ground, and polished with SiC paper and 1 µm diamond paste, and Au-coated. Ion microprobe analysis on the UCLA Cameca ims 1270 used a mass-filtered O^- (O refers to ^{16}O unless specifically noted) primary ion beam at ~60 nA and 22.5 keV impact energy, focused to a ~30 × 40 µm spot. Secondary ions were extracted at 10 kV with an energy bandpass of 50 eV and detected with a high-resistivity (10^{11} Ω) Faraday cup (FC) counting system for intensities >10^6 counts per second (cps) (typically for $^{232}ThO^+$ and $^{238}UO^+$) and with an ETP electron multiplier (EM) operated at ~2 kV for ion intensities <10^6 cps for all other masses. Count rates were corrected for EM dead time (25 ns) and FC baseline recorded on mass 247.5 during each measurement (~3 × 10^5 cps). FC-EM relative yields between 1.01 and 1.02 were determined from the ratio of measured $^{238}UO^+/^{235}UO^+$ to the $^{238}U/^{235}U$ atomic abundance ratio of 137.88 and used for correction of $^{230}ThO^+/^{232}ThO^+$ ratios.

$^{231}PaO^+$ molecular ions are ~10 times more abundant than $^{231}Pa^+$, similar to the behavior of U and Th atomic and molecular species in SIMS positive ion analysis of zircon. High-resolution mass spectra around mass 246 and 247 on natural zircons, synthetic cubic zirconia, hafnon, and the epoxy mounting medium indicate that a

* E-mail: axel@argon.ess.ucla.edu

mass resolving power m/Δm = ~4000 is sufficient to resolve the $^{197}Au^{18}OO_2^+$ and $^{197}AuO_3H_2^+$ interferences from $^{231}PaO^+$ (Fig. 2). Unresolved isobaric interferences such as $^{230}Th^{17}O^+$ and $^{230}ThOH^+$ are insignificant due to low abundances of the calculated peaks based upon the 246 amu mass region. Zirconium oxide molecular ion peaks (Fig. 2) were used for calibrating the magnetic field settings for low abundance isotopes and background mass stations at the beginning of each analysis and after every 15 cycles; on more intense peaks the magnetic field settings were calibrated directly in the same intervals. The abundance sensitivity at mass 247 due to the $^{232}ThO^+$ peak (~250 ppb measured on synthetic thorite) contributes to the background at mass 247.03 and intensities recorded at 247.1 amu were subtracted from the $^{231}PaO^+$ peak (Table 1). At a sputter rate of ~0.05 μm³/s/nA O^-, approximately 30 ng of zircon or 0.3 fg of Pa are consumed during a typical 30 min analysis. This corresponds to a useful yield (atoms detected over atoms sputtered) for $^{231}PaO^+$ in zircon of ~0.92%, similar to the useful yield determined for $^{230}ThO^+$ (~1.04%).

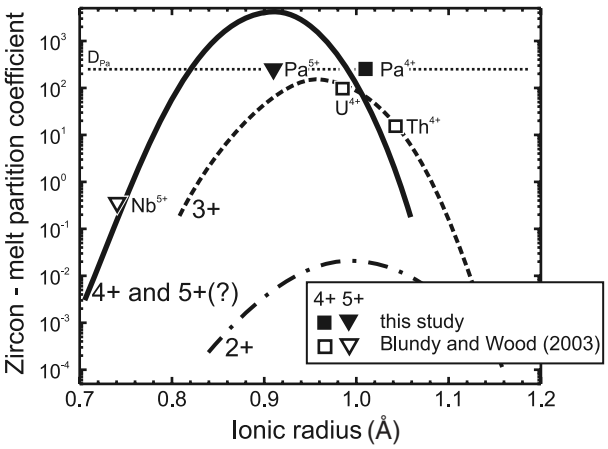

FIGURE 1. Lattice strain model for zircon-melt partitioning with curves for 4+ (solid), 3+ (dash), and 2+ (dash-dot) cations (after Blundy and Wood 2003). Model D_{Pa} (this study; uncertainty equivalent to size of symbols—see text) is plotted against ionic radius for Pa^{4+} and Pa^{5+} (VIII-coordination) using $D_U = 100$. Tetravalent D_{Th} and D_{Pa} both slightly deviate from the 4+ curve, whereas D_{Pa} for Pa^{5+} is more than 10× lower than predicted from using D_{Nb} as a proxy.

RESULTS

Relative sensitivity calibration on Buff Peak zircon (BP-1)

Relative sensitivity for Th/U species in SIMS is commonly calibrated by analyzing radiogenic $^{208}Pb/^{206}Pb$ on a concordant zircon with known age (Reid et al. 1997). Because a separate Pa-Pb decay system is non-existent and Pa-zircon standards are unavailable, the instrumental mass fractionation was determined from measuring the ratio of $^{231}PaO^+ \times \lambda_{231}$ over $^{235}UO^+ \times \lambda_{235}$ on a secular equilibrium reference zircon with $(^{231}Pa)/(^{235}U) = 1$ (λ refers to decay constant). Reference zircons were extracted from the 14.57 Ma ($^{40}Ar/^{39}Ar$ sanidine single-crystal age) Buff Peak tuff (Nevada), a rhyolite with ~20 ppm U, which is among the highest bulk rock U abundances for volcanic rocks in the Western U.S.A. (Castor and Henry 2000). Buff Peak zircons (BP-1) are homogenous in back-scatter electron imaging, except for occasionally intergrown thorite domains, which were avoided. Their high U abundance (~1–4 wt% UO_2) and comparatively high U/Th (~2.7–4.8) are favorable for ^{231}Pa analysis (Table 1).

TABLE 1. Ion microprobe U-series results for secular equilibrium reference zircons (BP-1, AS-3) and Salton Buttes rhyolite zircons

Zircon	grain*	spot	$(^{230}Th)/(^{238}U)$	$(^{238}U)/(^{232}Th)$	$(^{230}Th)/(^{232}Th)$	$(^{231}Pa)/(^{235}U)$	246.038/246.3	247.031/247.1	247.031 (cps)	UO_2 (wt%)
secular equilibrium (wt%)										
BP-1†	m1g2	1	1.012 ± 0.012	8.233 ± 0.082	8.334 ± 0.051	–	617	–	–	3.08‡
BP-1	m1g2	2	1.019 ± 0.014	8.470 ± 0.086	8.631 ± 0.086	1.047 ± 0.074	591	4.60	5.21	3.23‡
BP-1	m1g3	1	0.985 ± 0.015	11.13 ± 0.12	10.97 ± 0.11	1.042 ± 0.067	1112	5.36	5.36	1.77‡
BP-1	m1g4	1	0.985 ± 0.017	14.66 ± 0.15	14.43 ± 0.20	0.916 ± 0.075	859	5.41	2.41	0.87‡
BP-1	m1g5	1	0.974 ± 0.018	11.72 ± 0.13	11.41 ± 0.16	1.012 ± 0.068	805	5.18	4.89	1.64‡
BP-1	m1g6	1	0.993 ± 0.013	12.60 ± 0.13	12.51 ± 0.10	1.098 ± 0.070	1316	5.48	5.22	1.49‡
BP-1	m1g7	1	0.976 ± 0.022	10.09 ± 0.18	9.850 ± 0.133	0.894 ± 0.062	1566	3.19	6.16	1.79‡
BP-1	m2g1	1	0.985 ± 0.011	9.389 ± 0.076	9.248 ± 0.065	0.972 ± 0.065	1039	3.58	7.09	3.07
BP-1	m2g2	1	0.976 ± 0.011	12.10 ± 0.10	11.81 ± 0.09	1.029 ± 0.065	818	3.96	6.32	3.96
BP-1	m2g3	1	0.978 ± 0.010	10.23 ± 0.09	10.00 ± 0.06	0.905 ± 0.062	485	3.77	7.48	3.35
BP-1	m2g4	1	1.017 ± 0.010	9.142 ± 0.071	9.298 ± 0.06	1.110 ± 0.068	593	4.59	8.34	2.99
										U (ppm)
AS-3	m1g2	1	0.964 ± 0.017	4.532 ± 0.045	4.369 ± 0.064	1.113 ± 0.166	124	2.02	0.36	490
Salton Buttes										
SB0402§	m1g3	1	0.313 ± 0.024	4.783 ± 0.077	1.497 ± 0.112	3.281 ± 0.672	36.8	2.51	0.40	1150
SB0402	m1g1	1	0.237 ± 0.022	5.833 ± 0.065	1.385 ± 0.130	2.008 ± 0.535	14.8	1.98	0.29	240
SB0402	m1g4	1	0.269 ± 0.015	5.483 ± 0.113	1.475 ± 0.079	2.011 ± 0.375	32.6	4.56	0.45	570
SB0401‖	m2g1	1	0.272 ± 0.012	4.865 ± 0.048	1.324 ± 0.057	2.180 ± 0.337	272	4.14	0.85	1650
SB0401	m2g3	1	0.320 ± 0.017	5.011 ± 0.051	1.605 ± 0.083	2.344 ± 0.489	22.2	3.79	0.33	490
SB0402	m2g1	1	0.262 ± 0.018	5.412 ± 0.055	1.420 ± 0.096	1.802 ± 0.465	31.2	2.40	0.34	590
SB0402	m2g2	1	0.213 ± 0.025	7.226 ± 0.099	1.538 ± 0.182	3.776 ± 1.139	15.5	6.09	0.30	340
SB0402	m2g4	1	0.258 ± 0.021	6.241 ± 0.050	1.610 ± 0.133	2.562 ± 0.878	28.5	3.21	0.29	430
SB0401	m2g4	1	0.273 ± 0.014	5.156 ± 0.093	1.407 ± 0.067	1.787 ± 0.706	37.2	4.00	0.32	580
SB0401	m2g2	1	0.395 ± 0.010	2.834 ± 0.032	1.120 ± 0.025	1.536 ± 0.186	77.1	2.45	1.66	2940

Note: Activities in parentheses; decay constants used: $\lambda 235 = 9.8485 \times 10^{-10}\ a^{-1}$; $\lambda 231 = 2.1158 \times 10^{-5}\ a^{-1}$; $\lambda 238 = 1.55125 \times 10^{-10}\ a^{-1}$; $\lambda 230 = 9.1580 \times 10^{-6}\ a^{-1}$; $\lambda 232 = 4.9475 \times 10^{-11}\ a^{-1}$ (compiled in Bourdon et al. 2003). All errors 1σ (including measurement and RSF uncertainties) 246.038: peak $^{230}ThO^+$; 246.3: background $^{230}ThO^+$; 247.031: peak $^{231}PaO^+$; 247.1 background $^{231}PaO^+$.

* m1 analyzed August 22, 2006, (RSF Th/U = 0.908±0.009; RSF Pa/U = 0.782±0.020; RSF U/Zr = 0.02); m2 analyzed August 30, 2006, (RSF Th/U = 0.908±0.007; RSF Pa/U = 0.783±0.023; RSF U/Zr = 0.014); relative sensitivity factor (RSF) Th/U from $^{208}Pb/^{206}Pb$ analysis of 91500 zircon; RSF Pa/U from BP-1; (231Pa)/(235U) of BP-1 only shown as indication of reproducibility U/Zr RSF from $^{238}UO^+/^{90}Zr_2O_4^+$ on 91500 (81.2 ppm U).

† Sample location: N 41°21′37.1″; W 118°19′21.2″.

‡ Electron microprobe analysis (in wt%): SiO_2 = 30.4–31.1; P_2O_5 = 0.23–0.62; Y_2O_3 = 1.45–2.65; ZrO_2 = 57.4–61.3; HfO_2 = 1.59–1.90; ThO_2 = 0.29–1.04; UO_2 = 1.36–3.64; totals = 97.2–99.4.

§ SB0402 sampled at Obsidian Butte: N 33°10′14.6″; W 115°38′03.1″.

‖ SB0401 sampled at Red Island: N 33°11′59.1″; W 115°36′44.3″.

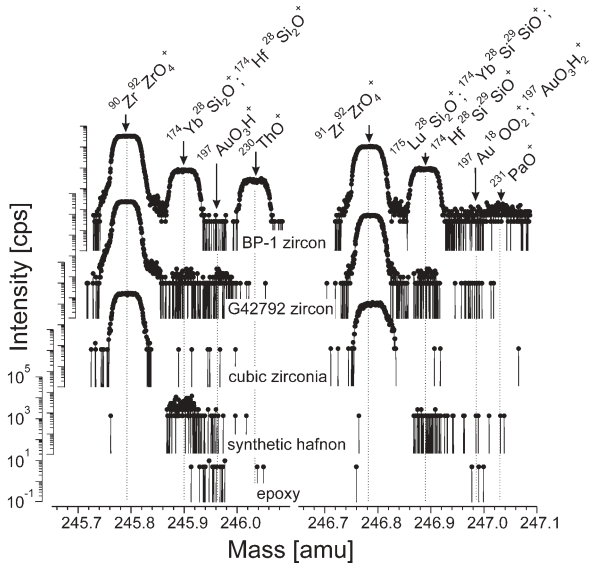

FIGURE 2. High-mass resolution spectra (m/Δm = 4500) of high-U zircon BP-1 (Buff Peak; ~3 wt% UO_2), low-U zircon G42792 (~24 ppm U), synthetic cubic zirconia, hafnon, and epoxy mounting medium.

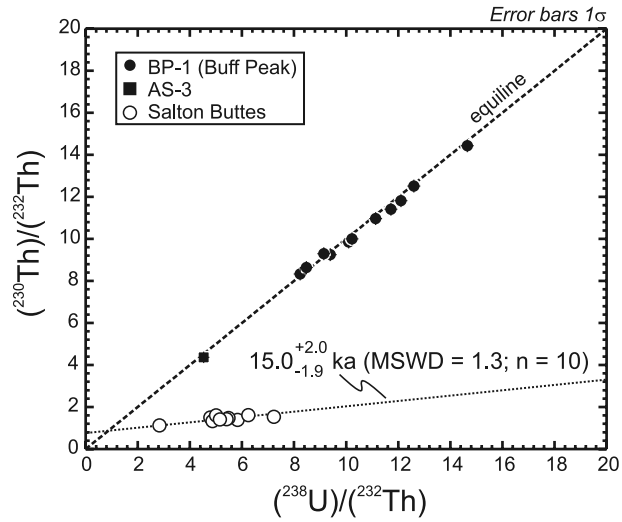

FIGURE 3. (^{230}Th)/(^{232}Th) vs. (^{238}U)/(^{232}Th) for equilibrium zircon crystals (BP-1, AS-3) and zircon crystals from the Holocene Salton Buttes. An error-weighted regression yields a ~15 ka isochron for zircon crystallization in the Salton Buttes rhyolite.

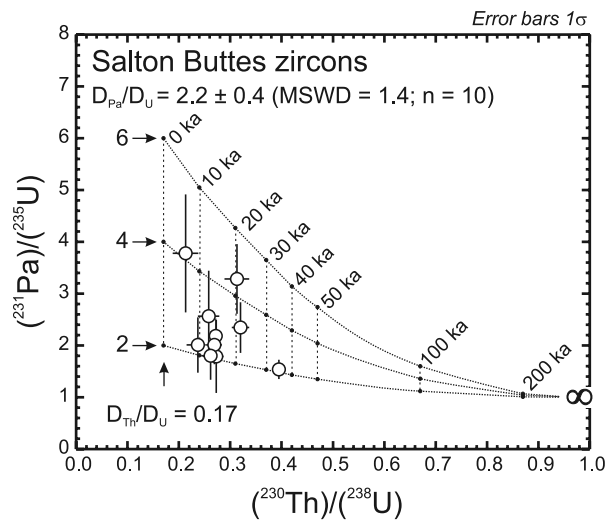

FIGURE 4. (^{231}Pa)/(^{235}U) vs. (^{230}Th)/(^{238}U) for Salton Buttes zircon crystals. Model activity ratio curves are drawn for zircon-melt partitioning with initial (^{230}Th)/(^{238}U) = D_{Th}/D_U = 0.17 (Blundy and Wood 2003) and (^{231}Pa)/(^{235}U) = D_{Pa}/D_U = 2, 4, and 6, respectively. Assuming U-series equilibrium in the melt, and correcting for the age of zircon crystallization (~15 ka), a weighted average model D_{Pa}/D_U of 2.2 ± 0.4 (1σ) is calculated.

U-series equilibrium of BP-1 zircon was verified by analyzing (^{230}Th)/(^{238}U) which was found to be in secular equilibrium (weighted average 0.992 ± 0.004; MSWD = 1.9; n = 10; all uncertainties 1σ; Fig. 3). The $^{231}PaO^+/^{235}UO^+$ relative sensitivity factor (RSF; measured ratio over true ratio) was 0.78 ± 0.02 (MSWD = 1.6; n = 10). RSF for ThO^+/UO^+ (0.91 ± 0.01; MSWD = 0.1; n = 3) was determined from $^{208}Pb^+/^{206}Pb^+$ on reference zircon 91500. To check RSF accuracy, a 105 cycle analysis (analysis time ~2 h) was performed on secular equilibrium zircon AS-3 and equilibrium values for (^{231}Pa)/(^{235}U) = 1.11 ± 0.17 and (^{230}Th)/(^{238}U) = 0.964 ± 0.017 were obtained (Table 1).

Pa-Th-U in zircons from Salton Buttes rhyolite

(^{231}Pa)/(^{235}U) and (^{230}Th)/(^{238}U) for ten individual spot analyses of zircon crystals from Salton Buttes are reported in Table 1 and plotted in Figure 4. Obsidian hydration dating of Salton Buttes rhyolite yielded an estimate for the eruption age of ~8.4 ka (Friedman and Obradovich 1981). The average zircon crystallization age from the Th-U isochron (Fig. 3) is $15.0^{+2.0}_{-1.9}$ ka (MSWD = 1.3). This closely agrees with previous SIMS zircon results by Schmitt and Vazquez (2006) who also reported Proterozoic zircon xenocrysts in the Salton Buttes lavas (excluded from age calculations). The weighted average of (^{231}Pa)/(^{235}U)$_{zircon}$ is 1.90 ± 0.13 (MSWD = 1.5; n = 10; Fig. 4). Using the average zircon crystallization age of 15 ka, average initial (^{231}Pa)/(^{235}U)$_{zircon}$ = 2.2 ± 0.2 (MSWD = 1.5) and (^{230}Th)/(^{238}U)$_{zircon}$ = 0.20 ± 0.01 (MSWD = 4.9) are calculated.

DISCUSSION

Initial (^{231}Pa)/(^{235}U)$_{zircon}$ can be translated into D_{Pa}/D_U provided that (^{231}Pa)/(^{235}U)$_{melt}$ is known. Unfortunately, measurements of (^{231}Pa)/(^{235}U)$_{melt}$ are unavailable for Salton Buttes rhyolites, but for other examples of intraplate silicic centers (Hekla, Iceland and Mono Craters, California) whole-rock (^{231}Pa)/(^{235}U) ranges between 1.17 and 1.19 (Pickett and Murrell 1997). Young ocean island and continental rift basalts typically have excess (^{230}Th)/(^{238}U) <1.6 that correlates roughly with (^{231}Pa)/(^{235}U) in proportions of 1:1.5 (Bourdon and Sims 2003; Lowenstern et al. 2006). Moreover, rhyolites in continental rift settings tend to have lower ^{230}Th excesses than associated basalts (Lowenstern et al. 2006). Considering that ^{231}Pa decays more than twice as fast as ^{230}Th, it is therefore reasonable to assume that (^{231}Pa)/(^{235}U)$_{melt}$ in rift rhyolites is likely between ~1 and 2.4. Within these limits for (^{231}Pa)/(^{235}U)$_{melt}$, model D_{Pa}/D_U values between 0.9 and 2.2 are

obtained for Salton Buttes zircon (Figs. 1 and 4).

The resulting model zircon-melt D_{Pa} for Pa^{5+} is much lower than predicted from its proxy D_{Nb} (Fig. 1; Blundy and Wood 2003). It is conceivable that this discrepancy is caused by an over-determination of Nb in zircon due to zirconium hydride interference (Blundy and Wood 2003). Interestingly, model D_{Pa} for Pa^{4+} plots closely to but not perfectly on the lattice strain curve for 4+ cations, leaving the possibility that Pa^{5+} species were insignificant in Salton Buttes rhyolite. Anomalously reduced magmatic conditions, however, can be ruled out based on characteristic positive Ce anomalies of Salton Buttes zircon (Ce/Ce* = 26–60; Schmitt and Vazquez 2006).

Regardless of Pa speciation, the detection of (^{231}Pa)/(^{235}U) disequilibrium in young zircon implies that Pa-U dating has the potential to establish relative crystallization sequences for late Pleistocene-Holocene (<150 ka) zircon if initial (^{231}Pa)/(^{235}U) was uniform for a suite of crystals in a rock, or yield absolute ages if the initial (^{231}Pa)/(^{235}U) can be independently constrained. The conclusion for U-Pb geochronology is that differences between concordant ^{207}Pb and excess ^{207}Pb (Δ^{207}Pb; Schärer 1984) caused by zircon-melt fractionation with D_{Pa}/D_U ~0.9–2.2 are vanishingly small for zircon older than a few ~tens Ma. Previous studies invoked much higher Δ^{207}Pb resulting from ^{231}Pa disequilibrium in zircon (e.g., ~100% for ca. 30 Ma zircons and ~5% for Archean zircons; Anczkiewicz et al. 2001; Parrish and Noble 2003). This would require initial ^{231}Pa excesses in the order of ~10^5–10^7%, instead of the maximum of ~200 % constrained by model D_{Pa}/D_U (Fig. 1). ^{207}Pb excesses in zircon—if valid—are therefore unlikely to result from zircon-melt fractionation alone and would require zircon crystallization in unrecognized reservoirs with extremely high (^{231}Pa)/(^{235}U).

Acknowledgments

Felix Wicke assisted in Buff Peak sampling and sample preparation. Frank Kyte helped in electron microprobe analysis. George Jarzebinski is thanked for technical support of the UCLA ion microprobe. Helpful comments by Kevin D. McKeegan, T. Mark Harrison, and journal reviewers Richard Stern, John W. Valley, and Anonymous are acknowledged. The ion microprobe facility at UCLA is partly supported by a grant from the Instrumentation and Facilities Program, Division of Earth Sciences, National Science Foundation

References cited

Anczkiewicz, R., Oberli, F., Burg, J.-P., Villa, I.M., Günther, D., and Meier, M. (2001) Timing of normal faulting along the Indus Suture in Pakistan Himalaya and a case of major ^{231}Pa/^{235}U initial disequilibrium in zircon. Earth and Planetary Science Letters, 191, 101–114.

Blundy, J. and Wood, B. (2003) Mineral-melt partitioning of uranium, thorium and their daughters. Reviews in Mineralogy and Geochemistry, 52, 59–123.

Bourdon, B. and Sims, K.W.W. (2003) U-series constraints on intraplate basaltic magmatism. In B. Bourdon, G.M. Henderson, C.C. Lundstrom, and S.P. Turner, Eds., Uranium-series Geochemistry, 52, p. 215–254. Reviews in Mineralogy and Geochemistry, Mineralogical Society of America, Chantilly, Virginia.

Bourdon, B., Turner, S., Henderson, G.M., and Lundstrom, C.C. (2003) Introduction to U-series geochemistry. In B. Bourdon, G.M. Henderson, C.C. Lundstrom, and S.P. Turner, Eds., Uranium-series Geochemistry, 52, 1–21. Reviews in Mineralogy and Geochemistry, Mineralogical Society of America, Chantilly, Virginia.

Castor, S.B. and Henry, C.D. (2000) Geology, geochemistry, and origin of volcanic rock-hosted uranium deposits in northwestern Nevada and southeastern Oregon, USA. Ore Geology Reviews, 16, 1–40.

Friedman, I. and Obradovich, J. (1981) Obsidian hydration dating of volcanic events. Quaternary Research, 16, 37–47.

Lowenstern, J.B., Charlier, B.L.A., Clynne, M.A., and Wooden, J.L. (2006) Extreme U–Th Disequilibrium in Rift-Related Basalts, Rhyolites and Granophyric Granite and the Timescale of Rhyolite Generation, Intrusion and Crystallization at Alid Volcanic Center, Eritrea. Journal of Petrology, 47, 2105–2122 (DOI: 10.1093/petrology/egl038).

Mattinson, J.M. (1973) Anomalous isotopic composition of lead in young zircons. Carnegie Institution of Washington Yearbook, 72, 613–616.

Parrish, R.R. and Noble, S.R. (2003) Zircon U-Th-Pb geochronology by isotope dilution; thermal ionization mass spectrometry (ID-TIMS). In J.M. Hanchar and P.W.O. Hoskin, Eds., Zircon, 53, p. 183–213. Reviews in Mineralogy and Geochemistry, Mineralogical Society of America, Chantilly, Virginia.

Pickett, D.A. and Murrell, M.T. (1997) Observations of ^{231}Pa/^{235}U disequilibrium in volcanic rocks. Earth and Planetary Science Letters, 148(1–2), 259–271.

Reid, M.R., Coath, C.D., Harrison, T.M., and McKeegan, K.D. (1997) Prolonged residence times for the youngest rhyolites associated with Long Valley Caldera; ^{230}Th-^{238}U ion microprobe dating of young zircons. Earth and Planetary Science Letters, 150(1–2), 27–39.

Schärer, U. (1984) The effect of initial ^{230}Th disequilibrium on young U-Pb ages; the Makalu case, Himalaya. Earth and Planetary Science Letters, 67, 191–204.

Schmitt, A.K. and Vazquez, A.J. (2006) Alteration and remelting of nascent oceanic crust during continental rupture: Evidence from zircon geochemistry of rhyolites and xenoliths from the Salton Trough, California. Earth and Planetary Science Letters, 252, 260–274.

Wilde, S.A., Valley, J.W., Peck, W.H., and Graham, C.M. (2001) Evidence from detrital zircons for the existence of continental crust and oceans on the Earth 4.4 Gyr ago. Nature, 409(6817), 175–178.

Manuscript received September 15, 2006
Manuscript accepted October 25, 2006
Manuscript handled by Bryan Chakoumakos